Rev. Adv. Mater. Sci. 32 (2012) 61-67

NANOSCALE AMORPHIZATION NEAR CRACK TIPS IN DEFORMED NANOCRYSTALLINE AND ULTRAFINE-GRAINED SOLIDS

I.A. Ovid'ko[1,2] and A.G. Sheinerman[1,2]

[1] Institute of Problems of Mechanical Engineering, Russian Academy of Sciences, St. Petersburg 199178, Russia
[2] Department of Mathematics and Mechanics, St. Petersburg State University, St. Petersburg 198504, Russia

Received: September 29, 2012

Abstract. A theoretical model is suggested which describes nanoscale amorphization near crack tips in pre-cracked nanocrystalline and ultrafine-grained solids under a mechanical load. Within the model, the amorphization processes are associated with splitting transformations of grain boundary (GB) disclinations whose formation is initiated by GB sliding in a solid. The nanoscale amorphization carries local plastic deformation, releases in part high local stresses near crack tips and thus hampers crack growth in nanocrystalline and ultrafine-grained solids.

1. INTRODUCTION

Nanocrystalline and ultrafine-grained materials have specific structural features – very small sizes of grains and large amounts of grain boundaries (GBs) – responsible for their unusual deformation behaviors; see, e.g., [1–12]. In particular, nanocrystalline and ultrafine-grained materials are specified by very high strength and hardness values exceeding 2-10 times those of their coarse-grained counterparts; see reviews [1–7]. These mechanical characteristics are attractive for a range of structural applications of materials with nanocrystalline and ultrafine-grained structures. However, as with other high-strength solids, nanocrystalline and ultrafine-grained materials typically have low ductility and toughness limiting their use in technologies [1–7]. For instance, low toughness of nanoceramics serves as a critical parameter suppressing their wide applications as structural materials [1,2,6]. At the same time, there are several examples of large enough toughness exhibited by nanoceramics [13–20], and these examples motivate search for approaches to systematic fabrication of nanocrystalline and ultrafine-grained materials having simultaneously high strength and good fracture toughness. In the context discussed, it is highly interesting to identify and describe the toughening micromechanisms that operate in nanocrystalline and ultrafine-grained materials, with their specific structural features taken into account.

Following experimental data [21–24], local amorphization (crystal-to-glass transformation) represents one of the processes occurring in vicinities of crack tips and thereby influencing crack growth in conventional coarse-grained materials. These amorphization processes at crack tips are described as those related to either stress-induced shift in melting/amorphization temperature [21,22] or intense generation of a high density of vacancies [23] in local regions near crack tips. Also, following experimental data, computer simulations and theoretical models, the initially crystalline structures can be locally amorphized at very high stresses in solids free from cracks; see, e.g., [25–32]. Besides, in

Corresponding author: I.A. Ovid'ko, e-mail: ovidko@nano.ipme.ru

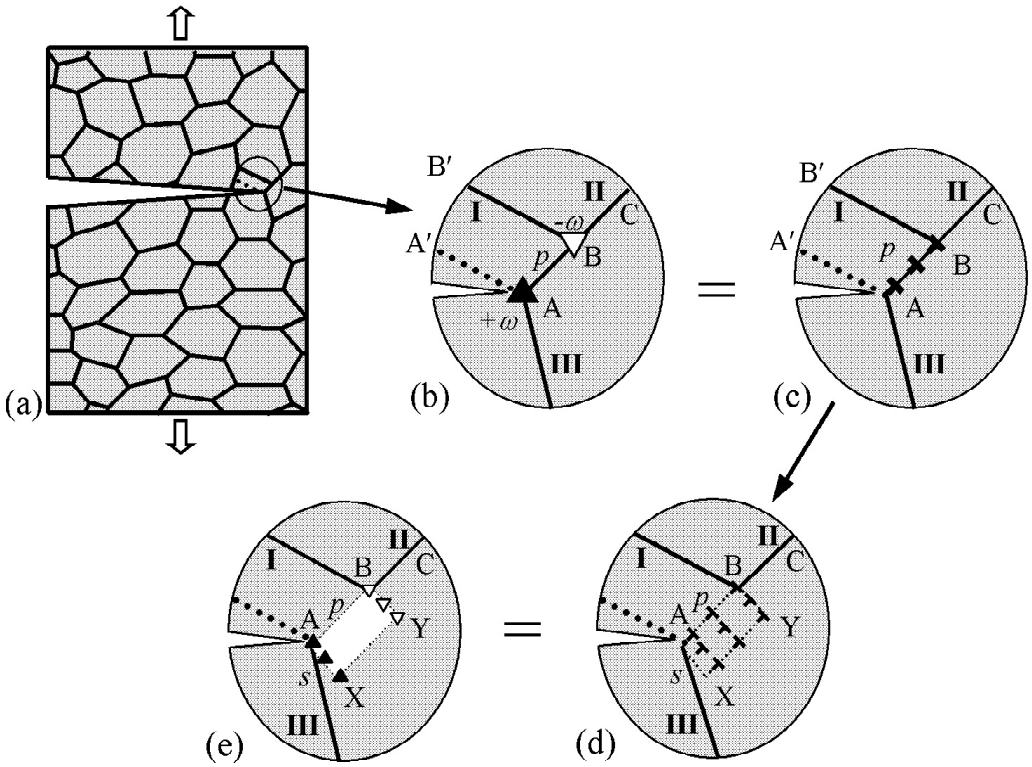

Fig. 1. Formation of an amorphous region around a disclination dipole near a crack tip in a nanocrystalline specimen deformed by grain boundary sliding. (a) General view. (b) Grain boundary sliding occurs along grain boundary II (AC) and results in transfer of both grain boundary I (from the position AA' to the position BB') and the triple junction (from the position A to the position B) over the distance *p*. Also, a disclination dipole (with the distance *p* between the wedge disclinations) is generated in the nanocrystalline specimen due to grain boundary sliding. (c) Disclination dipole AB is equivalent to the wall of edge grain boundary dislocations. (d) A rectangular amorphous region with the axes *s* and *p* forms around the wall of edge dislocations. Each dislocations delocalizes in the amorphous region, providing a uniform distribution of edge dislocations within this region. (e) The uniform distribution of edge dislocations in the amorphous region is equivalent to two distributions of disclinations of opposite strength, located at two opposite boundaries of the rectangular amorphous region.

the case of polycrystalline and nanocrystalline solids, theoretical analysis [33] and computer simulations [34] have demonstrated that nanoscale amorphization can effectively occur at GBs and their triple junctions as a process driven by relaxation of the elastic energy of GB disclinations (rotational defects) in the absence of any external mechanical load. With the experimental data [21–24] as well as the results of the theoretical model [33] and computer simulations [34], it is logical to expect that local amorphization processes at GB disclinations can come into play near crack tips in nanocrystalline and ultrafine-grained materials, where large amounts of GBs are present. The main aim of this paper is to suggest a theoretical model describing nanoscale amorphization processes near crack tips in deformed nanocrystalline and ultrafine-grained materials, with their specific structural features taken into consideration. Within our model, the amorphization processes carry local plastic deformation and are associated with splitting transformations of GB disclinations that result from GB sliding.

2. GEOMETRIC FEATURES OF NANOSCALE AMORPHIZATION PROCESSES NEAR CRACK TIPS IN NANOCRYSTALLINE AND ULTRAFINE-GRAINED SOLIDS

Let us consider a pre-cracked nanocrystalline solid consisting of nanoscale grains divided by GBs. Let the solid be under a remote tensile load and contain a mode I crack whose tip approaches a triple junction of GBs. A two-dimensional section of the solid is schematically shown in Fig. 1a. For the aims of this study, it is sufficient to use a two-dimen-

sional picture that captures physics of the amorphization process under our consideration.

GB sliding and other GB deformation mechanisms crucially contribute to plastic flow in nanocrystalline materials with finest grains (of sizes ≤20 nm) in wide temperature ranges [3–5]. Also, GB sliding serves as the dominant mode of superplastic deformation in nanocrystalline materials with intermediate grains (of sizes ranging from approximately 20 to 100 nm) and ultrafine-grained materials (having grain sizes in the range from approximately 100 to 1000 nm) at elevated temperatures [1,3,7]. As a corollary, GB sliding can play an essential role in nanoscale amorphization processes in nanocrystalline and ultrafine-grained materials during their (super)plastic deformation, and this aspect is involved in our model of such processes.

As to details, let us examine the situation where the external load concentrated at the crack tip induces GB sliding along one GB adjacent to the crack tip in a nanocrystalline or ultrafine-grained specimen (Fig. 1). Following [35–37], GB disclination dipoles typically form due to GB sliding. For instance, Fig. 1b schematically shows the transfer of a high-angle tilt boundary I (from the position AA' to the position BB') due to GB sliding along the high-angle boundary II (AC). In the initial state, the triple junction A of high-angle GBs is supposed to be geometrically balanced. (There is no angle gap at the triple junction A or, in other words, the sum of tilt misorientation angles at this triple junction is equal to zero.) As a result of transfer, the angle gaps ω and $-\omega$ appear at the GB junctions A and B, respectively (Fig. 1b), where ω is the tilt misorientation of the high-angle boundary I [38–40]. In the theory of defects in solids, the junctions A and B with the angle gaps $\pm\omega$ represent wedge disclinations which are characterized by the strengths $\pm\omega$ [41,42] and form a dipole configuration. Hereinafter we consider a GB disclination dipole produced by GB sliding, located near a triple junction of GBs and characterized by both the disclination strength ω and arm (the distance between disclinations) p (Figs. 1a and 1b). In other terms exploited in the theory of defects in solids [42], such a disclination dipole is equivalent to a finite wall of GB dislocations distributed between the points A and B (Fig. 1c).

We think that one of effective channels for relaxation of stresses created by the disclination dipole is the nanoscale amorphization associated with splitting transformations of GB dislocations, as it is schematically shown in Figs. 1c and 1d. More precisely, the GB dislocations move during their splitting transformations and thereby carry local plastic deformation (Figs. 1c and 1d). Since the GB dislocations are not lattice ones, their movement is accompanied by formation of a disordered region AXYB in the wake of the GB dislocations, as it is schematically shown in Fig. 1d. This disordered region is logically treated as the amorphous region. That is, in the case under our examination, the nanoscale amorphization occurs and serves as a special mode of plastic deformation (see also [32]). Its driving force is related to both a decrease in the elastic energy of the GB dislocations and the work of the plastic deformation carried by the GB dislocations during their splitting.

As to details, within our model, we consider a rectangular amorphous region AXYB with sizes s and p (Fig. 1d). For simplicity, as a first approximation, we assume that dislocations are continuously distributed over the amorphous region with a constant density (Fig. 1d). Although in practice, the density of dislocations in a specified point of the amorphous region should depend on the coordinate of this point with respect to the crack tip, our approximation significantly simplifies the calculations and, at the same time, gives us a rough estimate for the critical parameters of the amorphization.

The continuous uniform distribution of edge dislocations shown in Fig. 1d can be considered as an array of dislocation walls located between the opposite boundaries, AX and BY, of the amorphous region. In the theory of defects [42], each dislocation wall located between these boundaries is equivalent to a dipole of wedge disclinations. As a result, the uniform dislocation distribution over the amorphous region (Fig. 1d) is equivalent to the two uniform distributions of wedge disclinations over the boundaries AX and BY (Fig. 1e). (This equivalence is important for our examination, because it is convenient to use terms of disclinations in the calculations of the energy characteristics for the amorphization process.) The disclinations at the opposite boundaries AX and BY have opposite strength. Both distributions of the disclinations are characterized by the linear density $1/s$. The total strengths of the disclinations distributed over the boundary AX and BY are ω and $-\omega$, respectively (Fig. 1e).

Thus, the amorphization (associated with local plastic deformation) within a rectangular region around GB disclination dipole (Fig. 1e) is accompanied by the delocalization of the dipole of GB disclinations over two boundaries of the amorphous region. This scenario describes the nanoscale amorphization at GB disclination dipoles produced

by GB sliding in nanocrystalline and ultrafine-grained materials.

3. ENERGY CHARACTERISTICS OF NANOSCALE AMORPHIZATION PROCESSES NEAR CRACK TIPS IN NANOCRYSTALLINE AND ULTRAFINE-GRAINED SOLIDS

In order to reveal the conditions for the generation of the amorphous region around the disclination dipole (Fig. 1e), we calculate the energy change ΔW associated with its formation. The energy change ΔW can be presented as $\Delta W = W_2 - W_1$, where W_1 is the energy of the initial state (prior to the amorphization) (Fig. 1b), and W_2 is the energy of the final state containing an amorphous region (Fig. 1e). The formation of the amorphous region is energetically favorable, if $\Delta W < 0$. The energy change ΔW (per unit disclination length) can be represented as follows:

$$\Delta W = \Delta W_{\Delta} + \Delta W_{\Delta-\sigma} + W_{cg} - W_{gb} + W_{am}, \qquad (1)$$

where ΔW_{Δ} is the change of the disclination dipole energy due to the amorphization, $\Delta W_{\Delta-\sigma}$ is the change of the total energy of the interaction of the disclinations with the stress field created by the applied load near the crack tip, W_{cg} is the energy of the boundary between the crystalline and amorphous regions, W_{gb} is the energy of the GB fragments that disappear due to the amorphization, and W_{am} is the excess energy of the amorphous phase compared to the crystalline state.

In the following, we model the nanocrystalline specimen as an infinite elastically isotropic solid with the shear modulus G and Poisson's ratio ν and consider the crack as a semi-infinite one. In this case, one of the disclinations composing the dipole, by practice, is located at the crack free surface and does not create any stresses. As a corollary, the disclination dipole shown in Fig. 1b, in fact, represents a disclination. We also introduce two coordinate systems (x, y) and (x', y') with the origin at the crack tip (Fig. 2). Let the x-axis lie in the crack plane, the y'-axis correspond to the direction of GB sliding, and the x'-axis to the direction of the expansion of the amorphous nucleus (Fig. 2). Also, let the angle between the x- and x'-axes be equal to α. The energy variation ΔW_{Δ} can be represented as $\Delta W_{\Delta} = W_{dis} - W_{\Delta}$, where W_{dis} is the self-energy of the continuous distribution of the disclination dipoles in the solid with a crack, and W_{Δ} denotes the energy of the disclination of strength -ω, located near the crack tip, at the point (x'=0, y'=p).

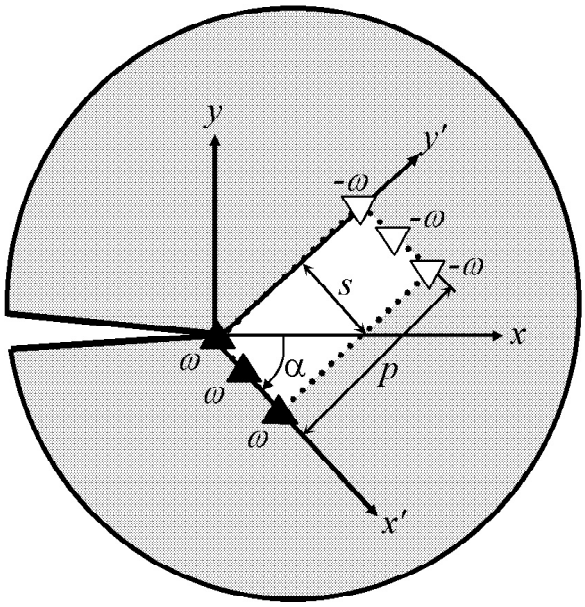

Fig. 2. Geometry of the amorphous region with disclinations near a crack tip.

The proper energy W_{Δ} of the disclination of strength -ω in an infinite isotropic solid with a semi-infinite crack can be written [43] as

$$W_{\Delta} = \frac{D\omega^2 p^2}{2} F(\alpha), \qquad (2)$$

where $F(\alpha)$ is the known function calculated in Ref. [43], and $D = G/[2\pi(1 - \nu)]$.

The energy W_{dis} of the distribution of disclination dipoles can be presented [44] in the form:

$$W_{dis} = -(1/2)\int_0^p \int_0^s \sigma^{dis}_{x'x'} \varepsilon^{*}_{x'x'}\, dx'\, dy', \qquad (3)$$

where $\sigma^{dis}_{x'x'}$ is the component of the stress field created by the distribution of the disclination dipoles, and $\varepsilon^{*}_{x'x'}$ is the eigenstrain created by this disclination distribution in the amorphous region. The stress $\sigma^{dis}_{x'x'}$ created by the distribution of the disclination dipoles is calculated using the expressions for the corresponding component $\sigma^{\Delta}_{x'x'}$ of the stress field created by the disclination of strength ω, located at the point ($x' = x'_0$, $y' = y'_0$), in a solid with a crack, as follows:

$$\sigma^{\Delta}_{x'x'}(x', y') = (1/s)\int_0^s \left(\sigma^{\Delta}_{x'x'}(x', y', x'_0, y'_0)\Big|_{y'_0=0} - \sigma^{\Delta}_{x'x'}(x', y', x'_0, y'_0)\Big|_{y'_0=p} \right) dx'_0. \qquad (4)$$

The eigenstrain $\varepsilon^{*}_{x'x'}$ created in the amorphous region by the distribution of the disclination dipoles is calculated using the expression [44] for the eigenstrain created by an individual disclination as

$$\varepsilon^{*}_{x'x'} = -\omega y'/s. \tag{5}$$

The expression for the stress $\sigma^{\Delta}_{x'x'}$ created by a disclination in an infinite isotropic solid with a flat semi-infinite crack is given [45] by

$$\sigma^{\Delta}_{x'x'} = \mathrm{Re}\left[4\Phi\cos^2\alpha - ge^{2/\alpha}\right], \tag{6}$$

where $g = \Phi + \overline{\Omega} + (z-\overline{z})\overline{\Phi}'$, and Φ and Ω are the complex potential of the disclination in the solid with a crack, $z = x + iy = (x' + iy')e^{-i\alpha}$ is the coordinate in the complex plane, and $i = \sqrt{-1}$. The expressions for the complex potentials are as follows [43]:

$$\Phi(z) = \frac{D\omega}{2}\left\{\ln\left(\sqrt{z}-\sqrt{z_0}\right) - \left(\sqrt{z}+\sqrt{\overline{z}_0}\right) + \frac{\sqrt{z_0}+\sqrt{\overline{z}_0}}{\sqrt{z}} + \frac{z_0-\overline{z}_0}{2\sqrt{z}\left(\sqrt{z}+\sqrt{\overline{z}_0}\right)}\right\}, \tag{7}$$

$$\Omega(z) = \frac{D\omega}{2}\left\{\ln\left(\sqrt{z}-\sqrt{z_0}\right) - \left(\sqrt{z}+\sqrt{\overline{z}_0}\right) + \frac{\sqrt{z_0}+\sqrt{\overline{z}_0}}{\sqrt{z}} + \frac{z_0-\overline{z}_0}{2\sqrt{z}\left(\sqrt{z}+\sqrt{z_0}\right)}\right\}, \tag{8}$$

where $z_0 = x_0 + iy_0 = (x_0' + iy_0')e^{-i\alpha}$ is the complex coordinate of the disclination.

Now the self-energy W_{dis} is calculated through the substitution of formulae (4)–(8) to formula (3), and the energy difference ΔW_{Δ} is computed using formulae (2)–(8) and the relation $\Delta W_{\Delta} = W_{dis} - W_{\Delta}$.

The energy change $\Delta W_{\Delta-\sigma}$ associated with the interaction of the disclination with the stress field created by the applied load in the solid with a crack is calculated using the known expression [43] for the interaction of the individual disclination with this stress field. The final expression for the energy change $\Delta W_{\Delta-\sigma}$ follows as

$$\Delta W_{\Delta-\sigma} = \frac{4\omega K_I}{3\sqrt{2\pi}}\left[(1/s)\int_0^s\left(x^{3/2}\cos^3\frac{\alpha}{2} - \left(x^2+p^2\right)^{3/4}\cos\frac{\mathrm{arccot}\left(x/p\right)-\alpha}{2}\right)\mathrm{d}x + p^{3/2}\cos^3\left(\frac{\pi}{4}-\frac{\alpha}{2}\right)\right], \tag{9}$$

where K_I is the stress intensity factor associated with the applied load.

The energy W_{cg} of the boundary between the amorphous and crystalline regions is calculated as

$$W_{cg} = 2\gamma_{cg}\left(s+p\right), \tag{10}$$

where γ_{cg} is the specific energy of the boundary. The energy W_{gb} of the GB segment of length p that disappears as a result of the formation of the amorphous region is given by

$$W_{gb} = \gamma_{gb}p, \tag{11}$$

where γ_{gb} is the GB specific energy. Finally, the energy W_{am} follows as

$$W_{am} = \Delta g_v sp, \tag{12}$$

where Δg_v is the specific (per unit volume) excess energy of the amorphous region.

Thus, we have derived the expressions for all the terms figuring in formula (1) for ΔW. Let us calculate ΔW for the case of nanocrystalline ceramic SiC. To do so, we will use the following parameter values typical for SiC: G = 217 GPa, ν = 0.23, $\gamma_{cg} = \gamma_{gb}$ = 0.5 J/m^2, and $\Delta g_v = 6.75\ 10^9$ J/m^3. We also put $\alpha = \pi/3$ and K_I = 1.3 MPA m$^{1/2}$. The chosen value of K_I corresponds to the theoretical estimate [43] for the SiC fracture toughness in the case of brittle fracture. Based on the results of Ref. [46], we calculated the equilibrium values of the length p of GB sliding for the above parameter values and various values of ω. The, we calculated ΔW for various values of s. It appeared that the formation of the amorphous region is energetically favored if its width s is smaller than some critical value s_c ($s<s_c$). The critical value s_c decreases with decreasing the disclination strength ω and rising the equilibrium length p of this region. Also, the dimensions of the amorphous region

are rather small. For example, at $\omega = 12°$ we have: $p \approx 4$ nm, $s_c \approx 1$ nm. The small dimensions of the amorphous region testify that amorphization in nanocrystalline solids at quasistatic loading can occur only in the nanoscale vicinities of crack tips, where the local stresses are very high.

4. CONCLUDING REMARKS

Thus, the nanoscale amorphization can occur at GB disclination dipoles (Fig. 1) and serve as a special mode of local plastic deformation near crack tips in nanocrystalline and ultrafine-grained solids under a mechanical load. Within our theoretical model presented in this paper, the amorphization processes are associated with splitting transformations of GB disclinations whose formation is initiated by GB sliding. The nanoscale amorphization in a pre-cracked solid carries local plastic deformation, provides strain energy relaxation and thereby hinders both the generation of nanocracks near the crack tip and the propagation of the pre-existent crack. To summarize, the stress-induced formation of nanoscale amorphous regions at GB disclination dipoles (Fig. 1) near crack tips plays the role as a toughening micromechanism capable of effectively contributing to increase in fracture toughness in nanocrystalline and ultrafine-grained solids.

ACKNOWLEDGEMENTS

The work was supported, in part, by the Russian Ministry of Education and Science (Contracts 14.740.11.0353 and 8025, and grant MD-164.2012.1) and the Russian Foundation of Basic Research (grant 12-01-00291-a).

REFERENCES

[1] R.Z. Valiev // *Nature Mater.* **3** (2004) 511.
[2] J.D. Kuntz, G.-D. Zhan and A.K. Mukherjee // *MRS Bull.* **29** (2004) 22.
[3] A. Mukhopadhyay and B. Basu // *Int. Mater. Rev*. **52** (2007) 257.
[4] M. Dao, L. Lu, R.J. Asaro, J.T.M. De Hosson and E. Ma // *Acta Mater.* **55** (2007) 4041.
[5] C.S. Pande and K.P. Cooper // *Progr. Mater. Sci.* **54** (2009) 689.
[6] I.A. Ovid'ko and A.G. Sheinerman // *Rev. Adv. Mater. Sci.* **29** (2011) 105.
[7] I.A. Ovid'ko and T.G. Langdon // *Rev. Adv. Mater. Sci.* **30** (2012) 103.
[8] R.Z. Valiev, I.V. Alexandrov, N.A. Enikeev, M.Yu. Murashkin and I.P. Semenova // *Rev. Adv. Mater. Sci.* **25** (2010) 1.
[9] A. Aronin, G. Abrosimova, D. Matveev and O. Rybchenko // *Rev. Adv. Mater. Sci.* **25** (2010) 52.
[10] E.D. Tabachnikova, A.V. Podolskiy, B. Bonarski, C. Mangler, V.Z. Bengus, S.N. Smirnov, A.N. Velikodny, M.A. Tikhonovsky and M.J. Zehetbauer // *Rev. Adv. Mater. Sci.* **25** (2010) 168.
[11] S.K. Mukhtarov, V.A. Valitov and N.R. Dudova // *Rev. Adv. Mater. Sci.* **25** (2010) 219.
[12] H. Garbacz, Z.Pakieła and K.J. Kurzydłowski // *Rev. Adv. Mater. Sci.* **25** (2010) 256.
[13] G.-D. Zhan and A.K. Mukherjee // *Int. J. Appl. Ceram. Technol.* **1** (2004) 161.
[14] Z. Xia, L. Riester, W.A. Curtin, H. Li, B.W. Sheldon, J. Liang, B. Chang and J.M. Xu // *Acta Mater.* **52** (2004) 931.
[15] S. Bhaduri and S.B. Bhaduri // *Nanostruct. Mater.* **8** (1997) 755.
[16] A.A. Kaminskii, M.Sh. Akchurin, R.V. Gainutdinov, K. Takaichi, A. Shirakava, H. Yagi, T. Yanagitani and K. Ueda // *Crystallography Reports* **50** (2005) 869.
[17] Y. Zhao, J. Qian, L.L. Daemen, C. Pantea, J. Zhang, G.A. Voronin and T.W. Zerda // *Appl. Phys. Lett.* **84** (2004) 1356.
[18] Y.T. Pei, D. Galvan and J.Th.M. De Hosson // *Acta Mater.* **53** (2005) 4505.
[19] R.W. Siegel, S.K. Chang, B.J. Ash, J. Stone, P.M. Ajayan, R.W. Doremus and L.S. Schadler // *Scr. Mater.* **44** (2001) 2061.
[20] H. Liu, C. Huang, X. Teng and H. Wang // *Mater. Sci. Eng.* A **487** (2008) 258.
[21] P.R. Okamoto, J.K. Heuer, N.Q. Lam, S. Ohnuki, Y. Matsukawa, K. Tozawa and J.F. Stubbins // *Appl. Phys. Lett*. **73** (1998) 473.
[22] M. Takeda, S. Ohnuki, P.R. Okamoto and N.Q. Lam // *J. Electron Microscopy* **48** (1999) 609.
[23] M. Nagumo, T. Ishikawa, T. Endoh and Y. Inoue // *Scr. Mater*. **49** (2003) 837.
[24] K. Youssef, P.K. Kuleshtha and G. Rozgonyi // *ESC Trans.* **25**, N 15 (2009) 49.
[25] H. Ikeda, Y. Qi, T. Cagin, K. Samwer, W.L. Johnson and W.A. Goddard III // *Phys. Rev. Lett.* **82** (1999) 2900.
[26] P.S. Branicio and J.P. Rino // *Phys. Rev.* B **62** (2000) 16950.
[27] E. Ma // *Scr. Mater.* **49** (2003) 941.

[28] X. Han, K. Zheng, Y.F. Zhang, X. Zhang, Z. Zhang and Z.L. Wang // *Adv. Mater.* **19** (2007) 2112.
[29] M. Peterlecher, T. Waitz and H.P. Karnthaler // *Scr. Mater.* **60** (2009) 1137.
[30] M. Chen, J.W. McCauley and K.J. Hemker // *Science* **299** (2003) 1563.
[31] X.Q. Yan, Z. Tang, L. Zhang, J.J. Guo, C.Q. Jin, Y. Zhang, T. Goto, J.W. McCauley and M.W. Chen // *Phys. Rev. Lett*. **102** (2009) 075505.
[32] I.A. Ovid'ko // *Scr. Mater*. **66** (2012) 402.
[33] M.Yu. Gutkin and I.A. Ovid'ko // *Philos. Mag. A* **70** (1994) 561.
[34] K. Zhou, A.A. Nazarov and M.S. Wu // *Phys. Rev. Lett.* **98** (2007) 035501.
[35] I.A. Ovid'ko and A.G. Sheinerman // *Appl. Phys. Lett.* **90** (2007) 171927.
[36] I.A. Ovid'ko and A.G. Sheinerman // *Acta Mater.* **57** (2009) 2217.
[37] I.A. Ovid'ko and A.G. Sheinerman // *Phys. Rev.* B **77** (2008) 054109.
[38] I.A. Ovid'ko, A.G. Sheinerman and E.C. Aifantis // *Acta Mater.* **56** (2008) 2718.
[39] W. Bollmann // *Philos. Mag.* A **49** (1984) 73.
[40] W. Bollmann // *Philos. Mag*. A **57** (1988) 637.
[41] M. Kleman and J. Friedel // *Rev. Mod. Phys.* **80** (2008) 61.
[42] A.E. Romanov and V.I. Vladimirov, In: *Dislocations in Solids*, ed. by F.R.N. Nabarro (North-Holland, Amsterdam, 1992), vol. **9**, p. 191.
[43] N.F. Morozov, I.A. Ovid'ko, A.G. Sheinerman and E.C. Aifantis // *J. Mech. Phys. Solids* **58** (2010) 1088.
[44] T. Mura, In: *Micromechanics of Defects in Solids* (Martinus Nijhoff Publishers, Dordrecht-Boston-Lancaster, 1987).
[45] A.C. Stevenson // *Proc. R. Soc.* A **184** (1945) 129.
[46] I.A. Ovid'ko, A.G. Sheinerman and E.C. Aifantis // *Acta Mater.* **59** (2011) 5023.